

# Experimental Study on Dielectric Relaxation in Alfa Fiber Reinforced Epoxy Composites

M. Arous,<sup>1</sup> I. Ben Amor,<sup>1</sup> S. Boufi,<sup>2</sup> A. Kallel<sup>1</sup>

<sup>1</sup>LaMaCoP, Faculté des Sciences de Sfax, BP 802-3018 Sfax, Tunisia

<sup>2</sup>LMSE, Faculté des Sciences de Sfax, BP 802-3018 Sfax, Tunisia

Received 15 November 2006; accepted 16 May 2007

DOI 10.1002/app.26885

Published online 29 August 2007 in Wiley InterScience (www.interscience.wiley.com).

**ABSTRACT:** Investigation on dielectric properties and behavior of thermoset epoxy composite based on cellulosic fibers has been carried on. Dielectric spectra were measured in the frequency range 0.1 Hz–100 kHz and at temperature intervals from ambient to 200°C. For the composite, four relaxations processes were identified, namely the orientation polarization imputed to the presence of polar water molecules in Alfa fiber, the  $\alpha$  mode relaxation associated with the glass transition of the epoxy resin matrix, the relaxation process associated with conductivity occurring as a result the carriers charges diffusion noted for high temperature above glass

transition and low frequencies, and interfacial or Maxwell-Wagner-Sillars relaxation that is attributable to the accumulation of charges at the Alfa fibers/epoxy resin interfaces. Dielectric relaxation analysis revealed evolution in water relaxation and it is thus concluded that the chemical treatment of the fiber can strongly influence the dielectrical properties and interfacial polarization processes in composites. © 2007 Wiley Periodicals, Inc. *J Appl Polym Sci* 106: 3631–3640, 2007

**Key words:** composites; charge transport; dielectric properties

## INTRODUCTION

Alfa fibers are extracted from the plant *Stippa tenacissima*, or esparto grass, and grows in the dry regions of North Africa and southern Spain.<sup>1</sup> This perennial grass, also named Esparto grass, is used as a main source of fiber for paper making. Paper produced from Alfa grass pulp, mixed with small amount of chemical wood pulp, is generally used in the manufacture of high quality printing papers and cigarette paper. Thanks to the short fiber length, the tensile strength of the paper is less than that of many other papers, but its resistance to shrinkage and stretching is superior. Likewise, the paper is well-filled, denser, and displays excellent inking qualities, and exhibit very good folding properties.<sup>2</sup>

Over the past decade there has been a growing interest in the use of lignocellulosic fibers as reinforcing elements for polymeric matrix.<sup>3–6</sup> The specific properties of this natural product, such as low cost, lightweight, renewable character, high specific strength and modulus, availability in a variety of forms throughout the world, reactive surface and the possibility to generate energy, without residue, after burning at the end of their life-cycle, motivate their association with organic polymers to elaborate com-

posite materials. These advantages, however, are reduced by the marked hydrophilic character of these macromolecules which, on one hand, limits their compatibility with widely used hydrophobic polymeric matrices such as polyolefins and, on the other hand, can reduce the mechanical properties of the composite if moisture is absorbed as they age.

Interfacial adhesion and resistance to moisture absorption of natural-fiber composites can be improved by suitable modification of fibers surface or by using coupling agents. Several strategies of surface modifications aiming at improving the compatibility between cellulose fibers and polymer matrices have been reported.<sup>7,8</sup> Many techniques have been used to gives evidence regarding the effect of the surface treatment on the fibers/matrix interfacial adhesion and to explore this region whose volume fraction does not exceed 1 up to 5 vol % of the composite. Among these techniques DMA (dynamic mechanical analysis) and SEM observation are the most employed. However, the recourse to other method able to probe the interface still attracts many interests and should help for better adapting the appropriate coupling agent according to the fiber's surface and the matrix.

Dielectric spectroscopy is one of the methods that are to give valuable information on the thermal and frequency behavior of polymer composites. When an electrical field is applied across a parallel-plate capacitor containing a dielectric, the various atomic and molecular charges present in the dielectric are

Correspondence to: M. Arous (Mourad.arous@fss.rnu.tn).

displaced from their equilibrium positions and the material is said to be polarized. Different polarization mechanisms can occur, including dipole orientation, extrinsic free charges or intrinsic charge migration, electrode polarization, and, in heterogeneous or composite systems, the Maxwell-Wagner-Sillars (MWS) interfacial polarization.<sup>9–11</sup>

Composites as a dielectric are becoming more popular and studies of electrical properties of natural fiber reinforced polymer composites are therefore very important. The electrical properties of some natural fibers, such as volume resistivity and dielectric strength have been studied by Kulkarni et al.<sup>9</sup> and there have been many studies of electrical properties of composites.<sup>10,11</sup> The electrical properties of epoxy matrix composites reinforced with sisal fiber have been studied by Chand and Jain<sup>12</sup> who analyzed the effects of temperature (24–180°C) and frequency (1–20 kHz) on the dielectric constant of matrix and composites. They found that the dielectric constant anisotropy ( $\epsilon'_{\text{transversal}}/\epsilon'_{\text{parallel}}$ ) and dielectric dissipation factor ( $\tan \delta$ ) of the epoxy and of sisal fiber epoxy composites decreases when the frequency increases.

Gravimetric and dielectric measurements have been used to monitor water uptake in composites with glass, jute, and washed jute fiber. Fraga et al.<sup>13</sup> showed that the dielectric constant of jute fiber composites is higher than that of the composites based on glass fibers which was imputed to higher hydrophilic character of jute fibers.

In the present work dielectric and conductivity relaxation have been used to explore the interfacial region of epoxy thermoset composite based on cellulose fibers and to investigate the effects of the fibers treatment by a reactive silane-coupling agent on the dielectric and interfacial MWS relaxation of the ensuing composite.

## EXPERIMENTAL

### Materials

#### Fiber treatment

Before the surface treatment, cellulose fibers in the form of sheets were soxhlet-extraction with ethanol for 24 h to remove contaminants or impurities on the surface of fibers. After the extraction, cellulose papers were placed in air to allow solvent to evaporate.

The treatment of cellulosic papers with 3% of silanes in weight was carried out in a 80/20 v/v ethanol/water at 2 h. Subsequently, the fibers were dried at room temperature for 2 days. Then the fibers were submitted to heat treatment at 110°C under moderate vacuum (1–2 mmHg for 1 h), to

ensure silane grafting on the fibers surface as reported in our previous work.<sup>14</sup>  $\gamma$ -aminopropyltriethoxysilane (APS) was a pure product from Aldrich. All other reagents and solvents were commercial products of the highest purity available.

#### Composite and specimen preparation

The handmade cellulose sheets were impregnated with epoxy liquid resin. The formulation used in the preparation of epoxy-based composites consisted of mixing 66.6 parts of EP resin and 33.4 parts of isophorone diamine as hardener. The resin mixtures were degassed before the sheet impregnation. To favor the complete wetting of the mat and to remove the air from within the fibers, the systems were kept under a vacuum of 10 mmHg for 15 min. The composites were then cured at 80°C for 1.5 h under a pressure of 2.5 MPa, and post cured at 140°C for 24 h to ensure thorough crosslinking of the matrix. The fibers loading on the composite is 40 vol %.

The EP resin (Epon 862) used was based on bisphenol diglycedylether with an epoxy index of 5.5, which corresponds to 170 g/equiv of epoxy functions. Its molecular weight was around 340. The crosslinking reactions were achieved with isophorone diamine (DA) using a molar stoichiometry of EP/DA = 1/1.8).

### Characterization

Dynamic mechanical tests were carried out with a RSA2 spectrometer from Rheometrics working in the tensile mode. The value of 0.05% for the strain magnitude was chosen to fall into the linear domain of viscoelasticity of the material. The samples were thin rectangular strips with dimensions of about  $30 \times 5 \times 0.5 \text{ mm}^3$ . Measurements were performed in isochronal conditions at 1 Hz, and the temperature was varied between 200 and 500 K at a rate of 3 K/min. This setup measured the complex tensile modulus  $E^*$ , i.e., the storage component  $E'$  and the loss component  $E''$  as well as the ratio between these two components ( $E'/E''$ ), i.e.,  $\tan \delta$ .

Dielectric determinations of the complex permittivity  $\epsilon^*$ , the real part (apparent permittivity)  $\epsilon'$ , the imaginary part (loss factor)  $\epsilon''$ ; and the dissipation factor  $\tan \delta$  ( $\tan \delta = \epsilon''/\epsilon'$ ) were performed on a dielectric thermal analyzer DEA 2970 from TA Instruments allowing measurements over the temperature range from –150 to 300°C and a frequency interval from 0.001 to 100 kHz. The samples were thin rectangular strips with dimensions of about  $10 \times 10 \times 0.5 \text{ mm}^3$ . The sample is placed between two gold parallel plate electrodes. The parallel plate sensors are used to evaluate bulk dielectric properties, and to track molecular relaxations. The lower elec-

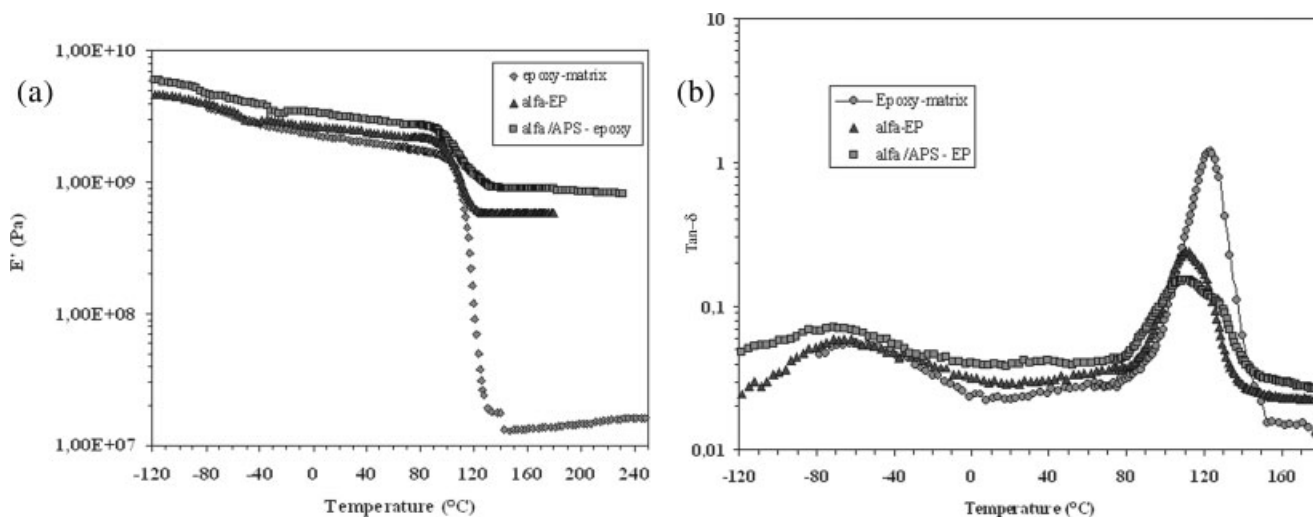


**Figure 1** Logarithm of the (a) storage tensile modulus  $\log E'$  and (b)  $\tan \delta$  at 1 Hz versus temperature for unfilled epoxy matrix, and both unmodified and modified Alfa reinforced composites containing 40% (v/v) fibers.

trode, positioned on the surface of the furnace, applies the voltage that sets up the electrical field in the sample. A platinum resistance temperature detector (RTD) surrounds the perimeter of the gold electrode and measures the temperature of the sample. The temperature is controlled directly by the RTD. The upper electrode, attached to the face of the ram, measures the generated current, which is then converted to an output voltage and amplified. A guard ring around the perimeter of the upper electrode corrects for electric field fringing and for stray capacitance at the edge of the plates. Signal circuits are connected through pads on the lower sensor, which contact spring probes attached to the ram. The plate spacing (sample thickness 0.5 mm) recorded at the start of the method is used throughout the experiment in the calculation of  $\epsilon'$  and  $\epsilon''$ . Two types of dielectric measurements were carried out: isochronal runs with fixed frequencies and ramping temperatures from ambient to 200°C, and then decreasing it, with a heating rate of 2°C/min in a nitrogen atmosphere on one hand, and isothermal runs with fixed temperature and scanning frequencies on the other hand.

## RESULTS AND DISCUSSION

### Dynamic mechanical analysis

The plot of the logarithm of the storage tensile modulus  $\log E'$  and  $\tan \delta$  at 1 Hz versus temperature for unfilled epoxy matrix, and both unmodified and modified Alfa reinforced composites containing 40% (v/v) fibers are shown on Figure 1(a,b), respectively. At low temperatures, the EP matrix is in the glassy state and  $E'$  remains roughly constant around 4.6 GPa. Then at  $\sim 100^{\circ}C$  a sharp drop in  $E'$ , by more

than 2.5 decades occurs, associated with the glass-rubber transition of the epoxy network. This relaxation phenomenon involves cooperative motions of long chain sequences which induce dissipation energy revealed by a maximum in  $\tan \delta$  [Fig. 1(b)]. Beyond this relaxation process, a rubbery plateau is attained which grows from 10 MPa for the unfilled matrix to about 600 MPa for the composite containing 40 vol % thus showing the reinforcing effect of the fibers. The fiber treatment by APS induced an increase in the modulus; both in its glassy and in its rubbery states, but the variations were more pronounced in rubbery region. Thus, at 20°C, the modulus increased from 2.55 GPa, for composites with untreated fibers, to 3.2 GPa for composites made with APS-treated fibers and at 150°C, a temperature higher than the  $T_g$  of the epoxy matrix, the corresponding modulus increased from 580 MPa to 900 MPa, respectively. The stronger reinforcing effect of the APS treated fibers was explained to the ability of the coupling agents to give rise to covalent bond continuity between the fibers and the epoxy matrix, which enhanced the interfacial bonding between the two phases and increased the efficiency of stress transfer between the matrix and the fibers. Figure 2 gives a schematic representation of the possible chemical reactions between the amino function of APS and the epoxy matrix during the hardening process. It is worth noting that improvement of the fiber-matrix adhesion after treatment by APS have been confirmed elsewhere by SEM observation.<sup>15</sup>

The evolution of the loss angle as a function of temperature [Fig. 1(b)] showed a secondary  $\beta$  relaxation around  $-70^{\circ}C$  ascribed according to Mangion and Johari to the relaxation of the hydroxyether units  $-O-CH_2-CH(OH)-CH_2-$  created during the crosslinking reaction of the epoxy prepolymer.<sup>16</sup>

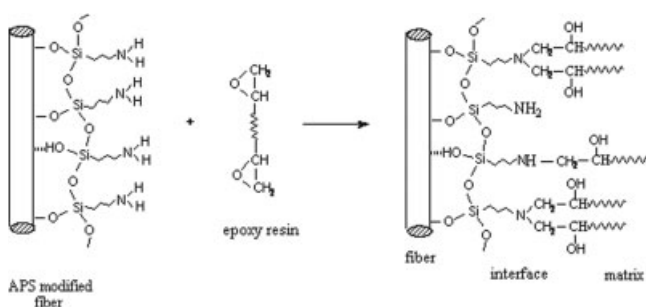


Figure 2 Schematic representation of interaction.

The  $\alpha$  relaxation associated with the glass transition of the matrix was detected at  $\approx 120^\circ\text{C}$ . Fibers incorporation in epoxy matrix did not lead to a detectable evolution of the glass transition. However, after the treatment with APS silane, the  $\alpha$  relaxation displayed a shoulder on the high temperature side of the main relaxation process, located around  $130^\circ\text{C}$  which may be associated with the rigid interfacial region where the epoxy chains display lower mobility as a result of a higher crosslink density in the vicinity of the fibers.

### Dielectric relaxation spectroscopy

#### Epoxy resin matrix

The dielectric characterization of the epoxy resin matrix was conducted from room temperature to  $\sim 200^\circ\text{C}$ . Figure 3 shows, respectively, the variation of the real part of the permittivity  $\epsilon'$  and the dissipation factor  $\tan \delta$  versus temperature for the following seven frequencies: 0.1, 1, 10, 100, 1000, 10,000, and 100,000 Hz. The real part of permittivity  $\epsilon'$  increased with temperature and was higher for the low frequency range [Fig. 3(a)]. Segmental mobility of the polymer molecules increased with temperature, leading to the increase in real part of the permittivity  $\epsilon'$ . In Figure 3(b), the epoxy resin matrix exhibits two maximum losses in low and high frequency domains.

- The first one emerging around 130, 150, and  $160^\circ\text{C}$  at  $10^3$ ,  $10^4$ , and  $10^5$  Hz, respectively, was attributed to the  $\alpha$  relaxation which is associated with the glass-rubbery transition of the polymer. The relaxation peak was shifted to high frequency when the temperature increased due to faster molecule movements leading to the decrease in the relaxation times.<sup>17</sup>
- The second one was attributed to ionic conduction appearing for temperatures above  $T_g$  and low frequency ranges (0.1 and 1 Hz), which arise from the increase in the mobility of electric charges in the polymer with temperature

thus giving rise to a conduction processes that bring about a large increase in both the real and imaginary part of the dielectric function.<sup>18–20</sup> For the epoxy resin  $-1$  slope of  $\epsilon''$ ; in the low frequencies region (Fig. 4) is typical for dc conductivity effect.<sup>21,22</sup> These results are confirmed by the corresponding ac conductivity plots for the epoxy resin (Fig. 5),  $\sigma_{ac}(f)$ , which exhibit a dc conductivity plateau at low frequencies and high temperatures. It is clear that dc conductivity is decreased and is shifted to the lower frequencies with temperature reduction which is an expected behavior due to the reduction in the carrier mobility.

### Composites

The loss factor  $\epsilon''$  and the dissipation factor  $\tan \delta$  versus frequency for the epoxy-based composites filled with unmodified Alfa fibers are shown in Figure 6, for different temperatures varying from 40 to  $200^\circ\text{C}$  in of  $10^\circ\text{C}$  increments. For low frequencies,

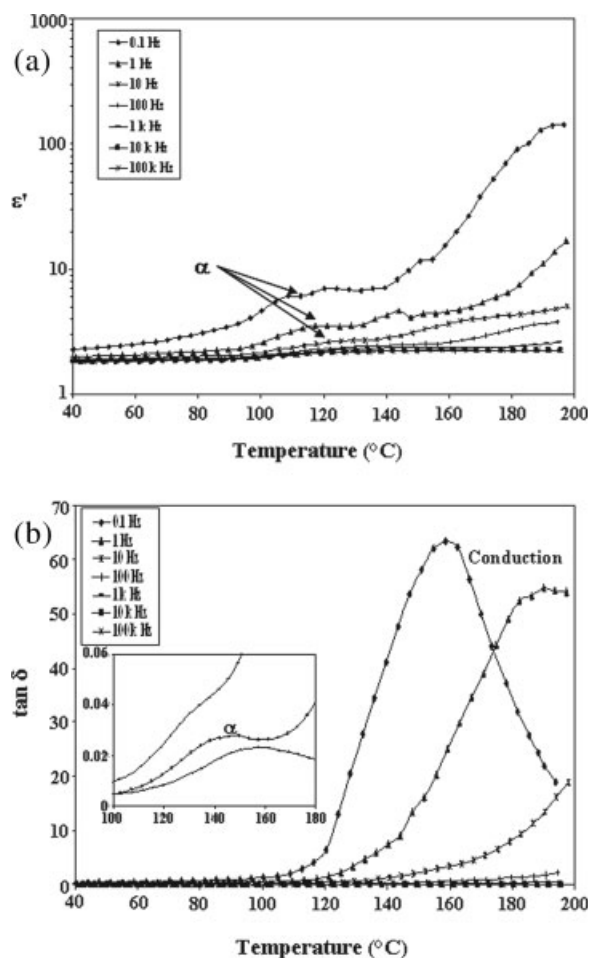
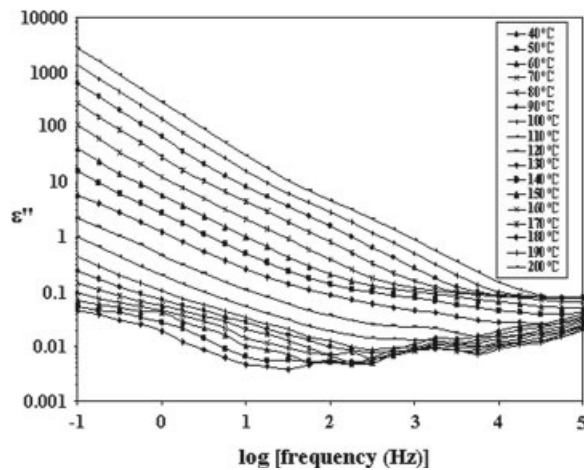


Figure 3 Isochronal runs of the real part of (a) the permittivity  $\epsilon'$  and (b) the dissipation factor  $\tan \delta$  as a function of temperature for the epoxy resin matrix.



**Figure 4** Isothermal runs of the loss factor  $\epsilon''$  versus frequency for the epoxy resin matrix.

the permittivity reached high values and achieved low values when frequencies increased. Compared to unfilled matrix incorporation of fibers brings about an amplification in the loss effect and gives rise to other relaxations in addition to one related to dc conductivity occurring in the low frequency and high-temperature domain (2 Hz at 190°C) Figures 6(b). In fact, the slope of  $\epsilon''$  (f) in this domain is  $-1$  which is typical for dc conductivity.<sup>23</sup>

The first one located at low temperature was associated to polarization of the water molecules linked to cellulosic fibers which formed a monomolecular layer wrapping the external surface of the fibers. Water molecules are known to be tightly bound to the surface hydroxyl groups of cellulose fibers and could not be removed irreversibly by a simple heat treatment.<sup>24</sup> Polar relaxation of water was equally pointed out by Chand and Jain in sisal composite based on epoxy or polyethylene matrix and was not completely vanished after different chemical treatment of cellulose fibers.<sup>12</sup> The second relaxation observed around 190°C at 6 Hz frequency was attributed to an interfacial polarization, known as the Maxwell-Wagner-Sillars (MWS) effect. This relaxation arises from the fact that free charges (catalysts, impurities, etc.), which were present at the stage of the processing, are now immobilized in the material. For temperatures high enough to ensure some conductivity of the media, the charges can migrate in the applied electrical field. These free carriers are then blocked at the interface between the cellulose fibers and epoxy matrix having differing permittivity and conductivity.<sup>25,26</sup> Indeed, at 150°C and for a frequency of 1 kHz, the permittivity and conductivity of the Alfa fibers is  $\sim 1.63$  and  $8.5 \cdot 10^{-12} \Omega^{-1} \text{cm}^{-1}$ , respectively, while it attained about 3.1 and  $5.5 \cdot 10^{-11} \Omega^{-1} \text{cm}^{-1}$  for epoxy matrix. It is worth to note that MWS is often confounded with ionic conduction as

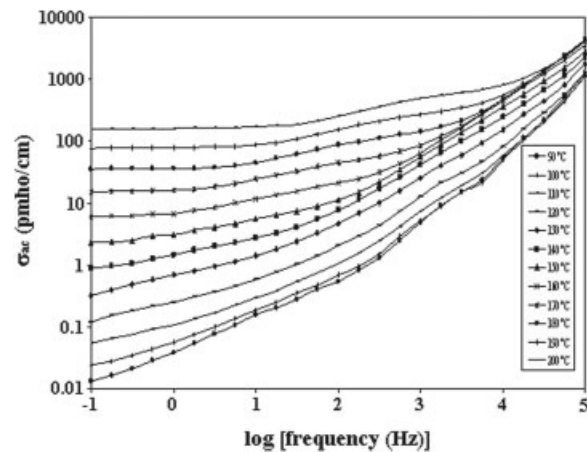


**Figure 5** Ac conductivity ( $\sigma_{ac}$ ) as a function of frequency for the pure epoxy resin at various temperatures.

these two phenomenons originate from charged carrier mobility.

The same trend is observed for composite based on silane treated Alfa fibers (Fig. 7). However, the

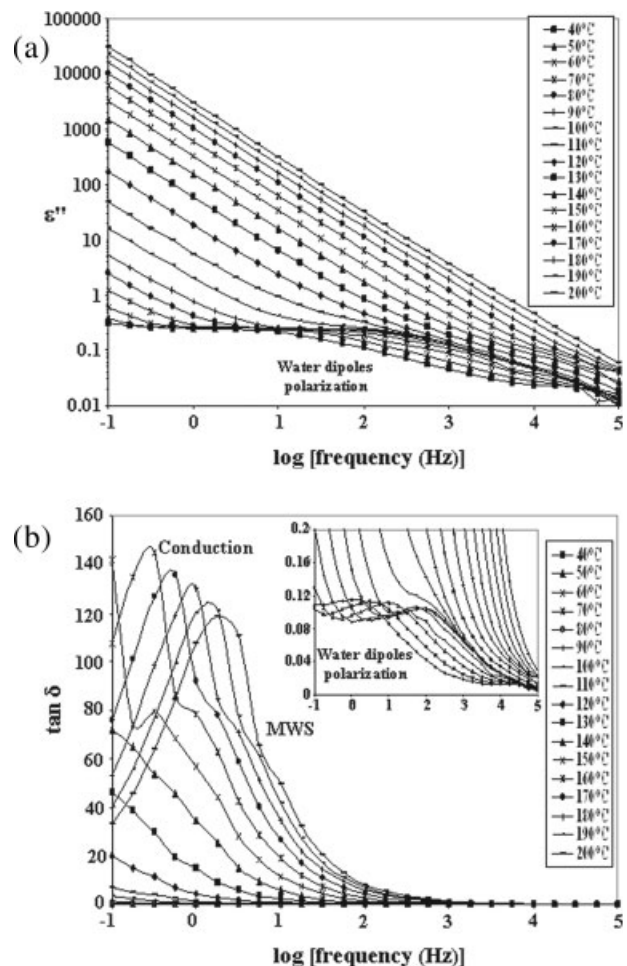


**Figure 6** Isothermal runs of (a) the loss factor  $\epsilon''$  and (b) the dissipation factor  $\tan \delta$  versus frequency for the epoxy resin filled with unmodified Alfa fibers.

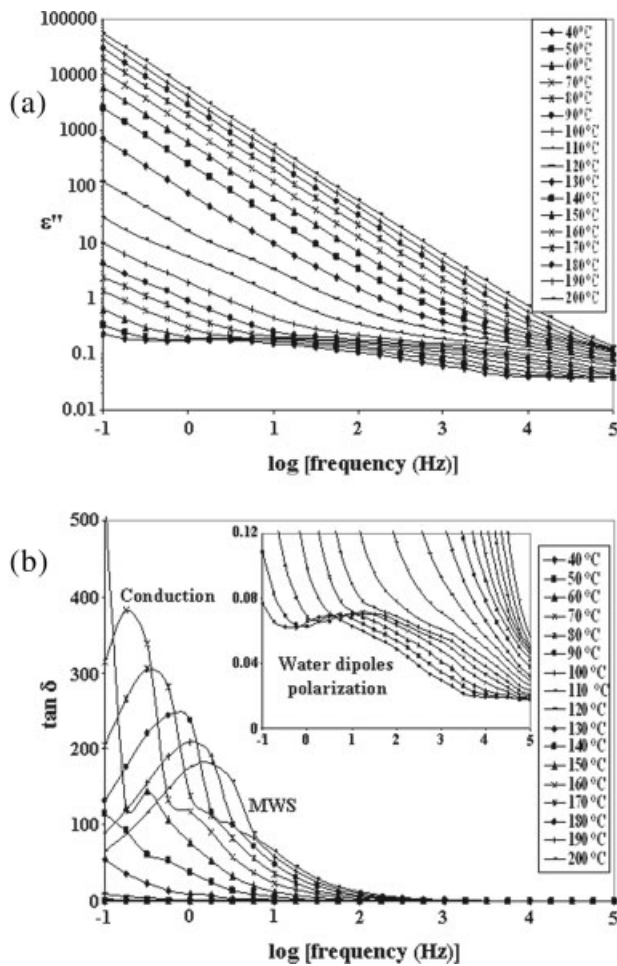


**Figure 7** Isothermal runs of (a) the loss factor  $\epsilon''$  and (b) the dissipation factor  $\tan \delta$  versus frequency for the epoxy resin filled with modified Alfa fibers.

relaxation associated with polar water molecules decreased in intensity, thus reducing the magnitude of  $\tan \delta$  compared to that relative to unmodified fibers. This phenomenon probably results from the decrease in the hydrophilic character of cellulose fibers after their treatment by APS silane which reduces in turn the amount of adsorbed water. The increase in the hydrophobic property of silane-treated fibers has been pointed out in a previous work where we showed that the contact angle of the fibers evolved from  $20^\circ$  for the pristine fibers up to  $60^\circ$  after treatment with APS.<sup>15</sup>

To minimize the effects of the dc conductivity, the formalism of "electric modulus" or "inverse complex permittivity" is introduced. This electric modulus has been recently adapted for the investigation of dielectric processes occurring in composite polymeric systems and also proposed for the description of systems with ionic conductivity.<sup>27,28</sup> In analogy to mechanical relaxation, the electric modulus  $M^*$  is defined by the following equation<sup>29</sup>:

$$M^* = \frac{1}{\epsilon^*} = \frac{1}{\epsilon' - j\epsilon''} = \frac{\epsilon'}{\epsilon'^2 + \epsilon''^2} + j \frac{\epsilon''}{\epsilon'^2 + \epsilon''^2} = M' + jM''$$

where  $M'$  is the real and  $M''$  the imaginary electric modulus.

The interest of the dielectric modulus formalism arises from the fact that in the case of the conductive processes that are observed at low frequencies, the loss factor exhibits a sharp monotonic increase whereas the imaginary part of the electric modulus show a peak. For that reason this function is the most suitable to study the space charge relaxation phenomena.

Adopting the electric modulus formalism, Figure 8 shows a noticeable difference between the epoxy resin and the composites. A series of three distinct relaxations can be considered as the sample is heated over the temperature range from 40 up to  $200^\circ\text{C}$ . The first of them is related to the orientation polarization of water dipoles. The second is the  $\alpha$  relaxation, assigned to the glass transition of polymer, and the third phenomenon is related directly to

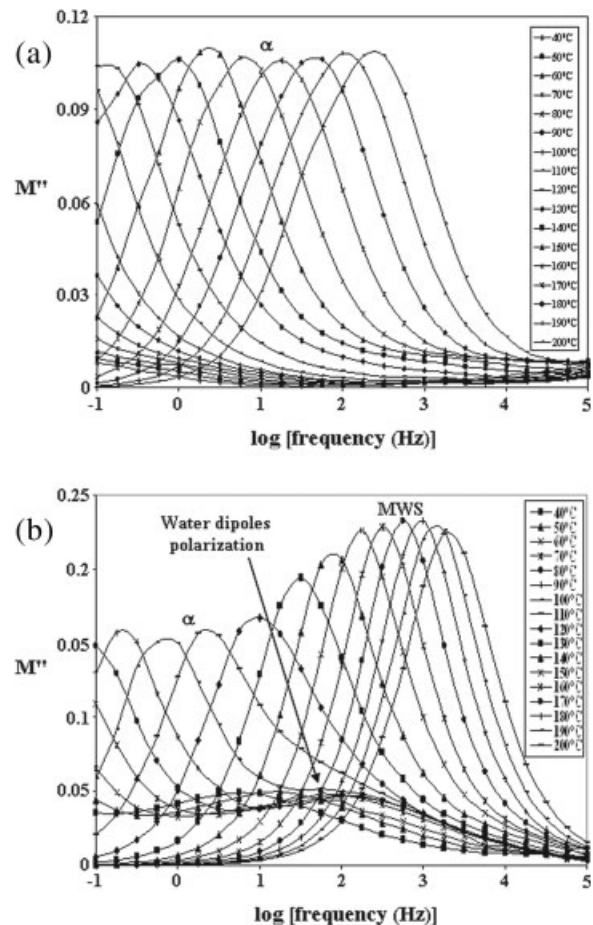


**Figure 8** The imaginary part  $M''$  of the electric modulus versus frequency of the epoxy resin filled with (a) 0% (v/v), (b) 40% (v/v) of unmodified alfa fibers.

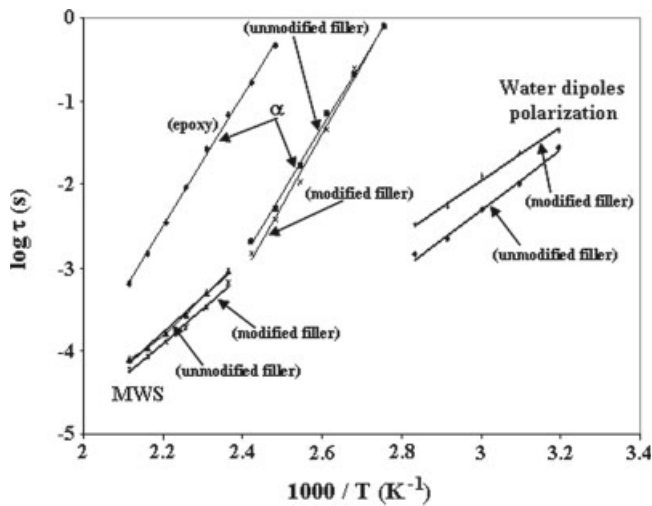


**Figure 9** Arrhenius plots of the relaxation times versus the reciprocal temperature for the epoxy resin filled with 0% (v/v), 40% (v/v) of unmodified and 40% (v/v) of modified Alfa fibers.

the filler or precisely to the fiber/matrix region giving rise to MWS interfacial polarization. To further support these assignments the activation energy relative to the different relaxation was evaluated using the Arrhenius relation  $\tau = \tau_0 \exp\left(\frac{E_a}{k_B T}\right)$

Where  $\tau = 1/2\pi f_{\max}$  is the relaxation time, which associated to the maximum of  $M''$  for a fixed temperature,  $E_a$  is the activation energy of the relaxation process,  $k_B$  is the Boltzmann constant, and  $T$  is the temperature. Figure 9 shows the evolution of  $\log(\tau)$  versus  $1/T$  for each of the different observed relaxation; i.e.,  $\alpha$  for epoxy matrix, and  $\alpha$ , MWS and water polarization for the composite based on untreated and treated cellulose fibers revealed that these three relaxation could be fitted with Arrhenius plot. Even though  $\alpha$  relaxation is better fitted with Vogel-Fulcher-Tamman (VFT), the apparent activation energy relative to this relaxation has been determined based on this model to compare them with the other relaxation.  $E_a$  and  $\tau_0$  are extracted, from the slopes and the intercepts of the plots  $\log \tau$  versus  $1/T$  (Fig. 9). The mean values of activation energy and  $\tau_0$  relative to water polarization and  $\alpha$  relaxation are 65 kJ/mol,  $10^{12.3}$  s and 154 kJ/mol,  $10^{-22}$  s, respectively (Table I). These value are in agreement with those reported in other work.<sup>21</sup> Likewise the MWS for the composite i.e., 80 kJ/mol for  $E_a$  and  $10^{-13.5}$  s for  $\tau_0$  is close to that reported for polystyrene-glass-bead composites.<sup>30,31</sup> Our values seem to be typical of a thermoactivated phenomenon related to elementary relaxations of dipoles as the characteristic times  $\tau_0$  is close to that of Debye ( $10^{-13}$  s). One can notice that apparent activation energy  $E_a^\alpha$  value associated to  $\alpha$  relaxation does not evolve after fibers incorporation, only after treatment by APS silane

coupling agent. The increase in  $E_a^\alpha$  could be rationalized if we consider that the amino groups attached to the grafted silane are able to react with epoxy cycle during the composite hardening. The ensuing reaction will improve the interfacial adhesion between the two phase and gives rise to a harder interfacial region as schematically illustrated in Figure 2 these hypothesis have been confirmed elsewhere using SEM observation.<sup>14</sup>

The use of the Argand representation (Cole-Cole diagram) provides interesting information regarding the nature of the relaxation. Cole-Cole plots of the epoxy resin matrix and the composite with untreated and treated Alfa fibers at 200°C are shown in Figure 10. The dotted curves are produced by best fitting experimental points to the Havriliak-Negami equation:<sup>32</sup>

$$\varepsilon^*(\omega) = \varepsilon_\infty + \frac{\varepsilon_s - \varepsilon_\infty}{(1 + (i\omega\tau)^\gamma)^\beta}$$

where  $\varepsilon_s$  and  $\varepsilon_\infty$  are the dielectric constants on the low- and high-frequency sides of the relaxation,  $\tau$  is the central relaxation time,  $\omega$  is the radial frequency, and  $\gamma$  and  $\beta$  are fractional shape parameters describing the skewing and broadening, respectively, of the dielectric function. Both  $\gamma$  and  $\beta$  ranges between 0 and 1. These coefficients act for the deviation from the Debye equation. In fact, when  $\gamma$  and  $\beta = 1$ , this equation reduces to the Debye equation.

In the electric modulus formalism the Havriliak-Negami equation have the following form:<sup>29</sup>

$$M' = \frac{\varepsilon'}{\varepsilon'^2 + \varepsilon''^2} = M_\infty M_s \frac{M_s D_1^2 + D_1 D_2 \cos \beta \phi}{M_s^2 D_1^2 + D_2 [D_2 + 2M_s D_1 \cos \beta \phi]}$$

$$M'' = \frac{\varepsilon''}{\varepsilon'^2 + \varepsilon''^2} = M_\infty M_s \frac{D_1 D_2 \sin \beta \phi}{M_s^2 D_1^2 + D_2 [D_2 + 2M_s D_1 \cos \beta \phi]}$$

**TABLE I**  
Activation Energies  $E_a$  and Relaxation Times  $\tau_0$  for Neat Matrix and Composite Materials

	$E_a$ (kJ/mol)	$E_a$ (eV)	$\tau_0$ (s)
Neat matrix			
$\alpha$ relaxation	150.0	1.55	$10^{-19.7}$
Unmodified filler			
Water dipoles relaxation	68.6	0.71	$10^{-13.0}$
$\alpha$ relaxation	150.8	1.56	$10^{-21.8}$
MWS relaxation	82.0	0.86	$10^{-13.2}$
Modified filler			
Water dipoles relaxation	61.6	0.64	$10^{-11.6}$
$\alpha$ relaxation	161.6	1.67	$10^{-23.3}$
MWS relaxation	78.2	0.81	$10^{-12.9}$

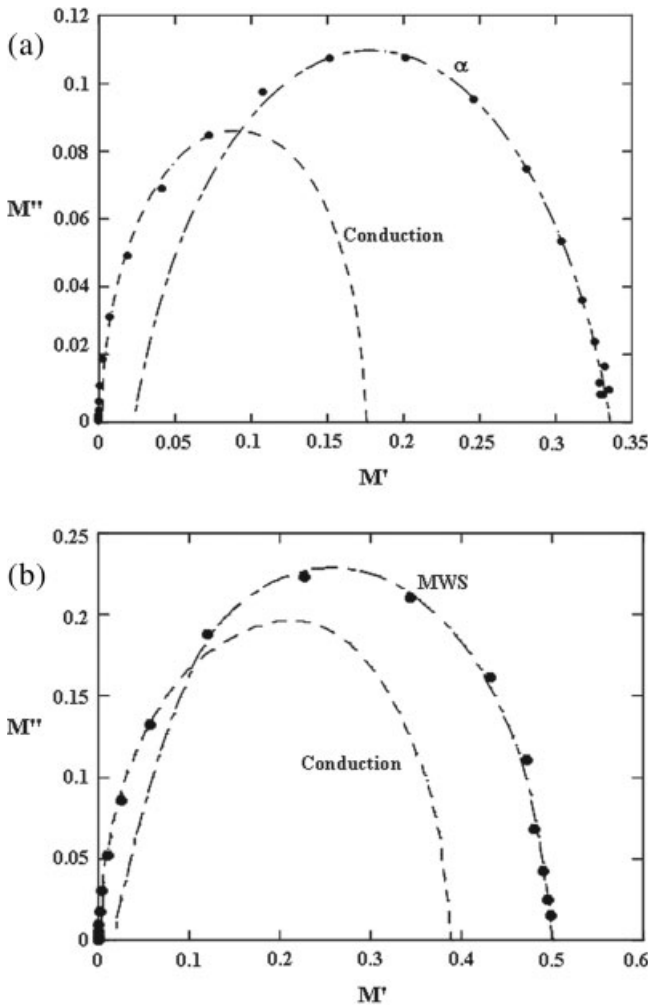


**Figure 10** Argand's plots of the electric modulus,  $M^*$  of (a) the epoxy resin and (b) the composites with unmodified Alfa fibers at 200°C. The dotted lines are produced by best-fitting the experimental points to the Havriliak-Negami approach.

Where  $M_s = 1/\varepsilon_s$ ;  $M_\infty = 1/\varepsilon_\infty$ ;  $D_1 = (\cos \varphi)^\beta [1 + (\omega\tau)^{2\gamma} + 2(\omega\tau)^\gamma \sin \frac{\gamma\pi}{2}]^\beta$

$$D_2 = (M_\infty - M_s) \left[ 1 + (\omega\tau)^\gamma \sin \frac{\gamma\pi}{2} \right]^\beta$$

$$(\omega\tau)^\gamma = \frac{\tan \left[ \frac{1}{\beta} \arctan \left[ \frac{M_\infty M''}{M_\infty M' - M''^2 - M'^2} \right] \right]}{\cos \frac{\gamma\pi}{2} - \sin \frac{\gamma\pi}{2} \tan \left[ \frac{1}{\beta} \arctan \left[ \frac{M_\infty M''}{M_\infty M' - M''^2 - M'^2} \right] \right]}$$

For the epoxy resin [Fig. 10 (a)] and at higher frequencies, the Cole-Cole diagram corresponds to the glass transition process. We note that it was impossible to fit the Havriliak-Negami model with all the experimental points. Likewise, one can notice that at the low frequency domain (lower values of  $M'$  and  $M''$ ) the experimental points reached the origin of the graph contrary to the theoretical ones which is a typical behavior dc conduction effect. For the com-

posite [Fig. 10 (b)], two semicircles are obtained in every examined temperature. The first for  $0 < M' < 0.1$  is related to the conduction effect and the second for  $0.05 < M' < 0.25$  is attributed to the MWS effect. The parameters evaluated by fitting data were listed in Table II. To determine the parameters characteristic of the model of Havriliak and Negami ( $\gamma$ ,  $\beta$ ,  $M_s$ ,  $M_\infty$ ), the experimental  $M'$  and  $M''$  data are smoothed through a numerical simulation in the complex plane. The purpose of such simulation is to find the theoretical values ( $M'_{th}$ ,  $M''_{th}$ ), which best fit, the experimental ( $M'_{exp}$ ,  $M''_{exp}$ ). The values of  $\gamma$ ,  $\beta$ ,  $M_s$ ,  $M_\infty$  which smoothed best the Havriliak Negami data are obtained by a successive approach method where the following expressions are minimized:

$$\chi_{M'}^2 = \sum_i (M'_{th} - M'_{exp})^2$$

$$\chi_{M''}^2 = \sum_i (M''_{th} - M''_{exp})^2$$

It has been verified that only one-quadruplet value is able to tune with these conditions.

Both for the MWS relaxation and conductive effect the value of  $\gamma$  and  $\beta$  agree with a pure Debye-type.<sup>33</sup> On the other hand, for water dipoles and  $\alpha$  relaxation, the deviation of  $\gamma$  value from 1 is an indication that these phenomena could not be associated to a single relaxation time process or a pure Debye-type relaxation.

Table III presents the Interfacial relaxation strength values defined by  $(\Delta\varepsilon = \varepsilon_s - \varepsilon_\infty)$ <sup>34</sup> as well as the values of the frequency at the maximum of relaxation MWS in permittivity form  $f_{max,\varepsilon}$ . The following relation gives the frequency of the maximum of the permittivity:<sup>29</sup>

$$f_{max,\varepsilon'} = \frac{M_s}{M_\infty} f_{max,M''}$$

The frequency of the maximum of the relaxation in electric modulus  $f_{max,M}$  is determined from the isothermal spectra of the imaginary part of the electric module  $M''$ . From Table III the following remarks could be pointed out:

- i. The frequency of the maximum of the interfacial relaxation is always lower than 200 Hz which could be an indication of the high contribution of ionic conduction which might hide MWS relaxation, thus justifying the use of the electric modulus in this study.
- ii. Relaxation strength increased with the temperature which can be due to the accumulation of



**TABLE II**  
Parameters Evaluated by Fitting Data According to the Havriliak-Negami Equation for Neat Matrix and Composite Materials

	$T$ (°C)	Relaxation	$\gamma$	$\beta$	$M_s$	$M_\infty$
Neat matrix	120	$\alpha$	0.73	0.98	0.037	0.374
	130	$\alpha$	0.77	0.96	0.022	0.335
	140	$\alpha$	0.82	0.96	0.02	0.316
	200	$\alpha$	0.79	0.98	0.022	0.336
Unmodified filler		Conduction	1	0.99	0.0012	0.176
	40	Water dipoles	0.49	0.94	0.318	0.567
	50	Water dipoles	0.52	0.88	0.336	0.581
	70	Water dipoles	0.57	0.82	0.357	0.578
	180	Conduction	1	1	0.00081	0.440
		MWS	1	0.98	0.023	0.504
	190	Conduction	1	1	0.00079	0.425
		MWS	1	0.98	0.018	0.505
	200	Conduction	1	0.99	0.00076	0.391
		MWS	1	0.96	0.016	0.501
Modified filler	40	Water dipoles	0.39	0.98	0.311	0.482
	50	Water dipoles	0.40	0.98	0.310	0.477
	70	Water dipoles	0.37	0.99	0.284	0.488
	180	Conduction	1	0.99	0.00061	0.350
		MWS	1	0.99	0.039	0.394
	190	Conduction	1	0.99	0.00058	0.354
		MWS	1	0.98	0.030	0.396
	200	Conduction	1	0.99	0.00053	0.328
		MWS	1	0.98	0.027	0.394

free charges at the interfaces, thus increasing the aptitude of the dipoles to be polarized. This phenomenon is amplified by temperature rise which accelerate the charge carrier mobility.

- iii. The treatment of the fibers leads to a significant increase by about 100 Hz in the maximum frequency relaxation. The same remark was observed for epoxy matrix reinforced by core-shell particles.<sup>35</sup> The authors showed that interfacial relaxation is affected by the more or less diffuse nature of the interface. For a "perfect" interface, because of high potential barrier there is no injection of charge carriers from the conductive phase to the less conductive phase where charge carriers are blocked and consequently the frequency of the maximum of MWS relaxation is increased.
- iv. The relaxation strength  $\Delta\epsilon$  decreased after the treatment with APS silane indicating a regidification of the fiber-matrix interfacial region

which in turn reduced the ability of dipole to relax. This result is in agreement with DMA analysis showing an increase in the storage modulus  $E'$  at a temperature higher than the  $T_g$  of the matrix. Similar trend was pointed out for polystyrene-glass-bead composite after coating of the filler with styrene-methacrylic acid copolymer which is expected to enhance the compatibility and the adhesion between PS matrix and glass bead.<sup>31</sup>

## CONCLUSIONS

In the present work investigation regarding the dielectric behavior of epoxy matrix and composites based on lignocellulosic alfa fibers, have been studied over the temperature range from room temperature to 200°C and over the frequency range from 0.1 Hz to 100 kHz. In addition to the  $\alpha$  relaxation associated to the glass transition of the epoxy resin matrix and ionic relaxation caused by the mobility of electric charges, the presence of cellulose fibers in the composite gives rise to other relaxation associated to water polarization and MWS interfacial polarization. The MWS relaxation arises from the trapping of electric charges at the interfaces between the Alfa fibers and the epoxy resin matrix. The treatment of the fibers with reactive silane coupling agent bearing amino group likely to react with the matrix leads to a decrease of the magnitude of water relaxation and increase the activation energy of  $\alpha$  relaxation which

**TABLE III**  
Interfacial Relaxation Strength as Well as the Values of the Frequency of the Maximum of Relaxation MWS

Composites	$T$ (°C)	$\Delta\epsilon$	$f_{\max,\epsilon''}$ (Hz)
Unmodified filler	180	41.5	43.6
	190	53.6	51.1
	200	60.5	63.5
Modified filler	180	23.1	120.4
	190	30.8	137.3
	200	34.5	181.0

have been explained (i) in term of the reduction in the hydrophilic character of the fibers and (ii) to ability of amino groups of the grafted silane to react with the matrix through the interfacial region, thus enhancing the fiber-matrix adhesion. Thanks to the high values of  $\epsilon''$ , which hid the MWS relaxation, data results was analyzed using the modulus formalism which is a very useful representation when conductivity processes are involved. Three relaxations were identified that are (i) water dipoles polarization, (ii) the  $\alpha$  relaxation, assigned to the glass transition of the matrix, and (iii) the MWS interfacial polarization. The recourse to the Argand representation confirmed that the later relaxation is consistent with a pure Debye process for the studied composites. Moreover, the maximum frequency relaxation of MWS relaxation is shown to be sensitive to the treatment with reactive silane coupling agent. Overall, the results pointed out the interest of dielectric spectroscopy as an additional technique that can be used to probe the composite interphase and investigate the effect of fibers treatment on the evolution of composite interfacial properties.

## References

1. Cerda, A. *J Arid Environ* 1997, 36, 37.
2. Ahrens, F. W.; Gulya, T.; Worry, G. L.; Walter, W. P. U.S. Pat. 853,547 (1998).
3. Plackett, D. Proceeding, Progress in Woodfiber-plastic Composites conferences, May 23–24 2000, Toronto, Canada.
4. Ellison, G. C.; McNaught, R. Proceeding of the natural fibres for the automotive industry conference, Actin, UMIST, Manchester, UK, Nov. 28 2000.
5. Rana, A. K.; Mandal, A.; Bandyopadhyay, S. *Compos Sci Technol* 2003, 63, 801.
6. Makki, A.; Boufi, S.; Belgacem, N.; Dufresne, A. *Compos Sci Technol* 2007, 67, 1627.
7. Laly, A. P.; Sabu, T. *Comp Sci Technol* 2003, 63, 1231.
8. Bisanda, E. T. N.; Anshell, M. P. *Compos Sci Technol* 1991, 41, 165.
9. Kulkarni, A. G.; Satyanarayana, K. G.; Rohatgi, P. K. *J Mater Sci* 1983, 18, 2290.
10. Paul, A.; Joseph, K.; Sabu, T. *Comp Sci Technol* 1997, 57, 67.
11. Sgriccia, N.; Hawley, M. C. *Comp Sci Technol* 2007, 67, 1986.
12. Chand, N.; Jain, D. *Compos A* 2005, 36, 594.
13. Fraga, A. N.; Frulloni, E.; De la Osa, O.; Kenny, J. M.; Vazquez, A. *Polym Test* 2006, 25, 181.
14. Abdelmouleh, M.; Boufi, S.; Ben Salah, A.; Belgacem, M. N.; Gandini, A. *Langmuir* 2002, 18, 3203.
15. Abdelmouleh, M.; Boufi, S.; Belgacem, N.; Dufresne, A.; Gandini, A. *J Appl Polym Sci* 2005, 98, 974.
16. Mangion, B. B. R.; Johari, G. P. *Macromolecules* 1990, 23, 3687.
17. Tsangaris, G. M.; Psarras, G. C.; Kontopoulos, A. J. *J. Non-Cryst Solids* 1991, 131, 1164.
18. Kyritsis, A.; Pissis, P.; Grammatikakis, J. *J Polym Sci Part B* 1995, 33, 1737.
19. Jonscher, A. K. *J Phys D: Appl Phys* 1999, 32, 57.
20. Schaumburg, G. *Novocontrol Dielectric Newslett* 1997, November, 8.
21. Kanapitsas, A.; Pissis, P.; Kotsilkova, R. *J Non-Cryst Solids* 2002, 30, 204.
22. Hammami, H.; Arous, M.; Lagche, M.; Kallel, A. *J. Alloys Compounds* 2007, 430 1/2,14, 1.
23. Psarras, G. C.; Manolakaki, E.; Tsangaris, G. M. *Compos A* 2002, 33, 375.
24. Roberts, J. C. *The Chemistry of Paper*; The Royal Society of Chemistry: Cambridge, 1996.
25. Tsonos, C.; Apekis, L.; Zois, C.; Tsonos, G. *Acta Mater* 2004, 52, 1319.
26. Perrier, G. *Recent Res Dev Polym Sci* 1999, 3, 175.
27. Wübbenhorst, M.; Turnhout, J. V. *J Non-Cryst Solids* 2002, 305, 40.
28. Hammami, H.; Arous, M.; Lagache, M.; Kallel, A. *Compos A* 2006, 37, 1.
29. Tsangaris, G. M.; Psarras, G. C.; Kouloumbi, N. *J Mater Sci* 1998, 33, 2027.
30. Perrier, G.; Bergeret, A. *J Appl Phys* 1995, 77, 2651.
31. Arous, M.; Kallel, A.; Fakhfakh, Z.; Perrier, G. *Comp Int* 1997, 5, 137.
32. Havriliak, S.; Negami, S. *J Polym Sci* 1996, 4, 99.
33. Howard, W.; Starkweather, J. R.; Avakian, P. *J Polym Sci B* 1992, 30, 637.
34. Puértolas, J. A.; Castro, M.; Telleria, I.; Alegria, A. *J Polym Sci B* 1999, 37, 1337.
35. Lestriez, B.; Maazouz, A.; Gérard, J. F.; Sautereau, H.; Boiteux, G.; Seytre, G.; Kranbuehl, D. E. *Polymer* 1998, 39, 6733.